Design and analysis of a scheme to mitigate condensation on an assembly used to cool a processor module

by M. J. Ellsworth, Jr. R. R. Schmidt D. Agonafer

System performance of an IBM RS/6000® workstation was improved by cooling to subambient temperatures the CMOS circuits of a single-chip module (SCM) mounted on a card. However, when refrigeration temperatures are sufficiently low, the temperature of all or a portion of the card on which the module is mounted can fall below the environmental dew point, resulting in unwanted condensation. Strategically placed heaters can maintain the temperature of the card surface above the dew point, but at the expense of increasing the total heat load the refrigeration unit must remove from the system. A 3D finite element analysis was used to investigate some of the key parameters that affect the thermal packaging design of a refrigeration-cooled low-temperature processor module with the objective of preventing condensation on exposed module card surfaces with minimal power input to the added heaters.

Introduction

There is a continuous need for increased performance from computer systems. Measurements¹ of the switching

Major semiconductor and computer companies have shown interest in this cooling technology during recent

0018-8646/02/\$5.00 © 2002 IBM

¹ A. Sutcliffe, unpublished results, IBM, Poughkeepsie, New York, October 9, 1998.

speed of a G5 system multichip module (MCM) that is populated with CMOS chips and mounted on a board showed that performance improves from 3.1% to 4.6% over the temperature range of 7°C to -20°C when the module is cooled with a liquid refrigerant. A 100°C temperature decrease in chip operating temperature may be achieved by using a vapor compression refrigeration cycle, thereby providing the potential for a system performance improvement of about 14%.2 In addition to improved performance, there are two other reasons for possible increased use of sub-ambient cooling of computer chips in the future. First, because many degradation mechanisms in electronic devices have a thermally activated component that is exponentially dependent on temperature, chip reliability is improved as the chip temperature is lowered. However, because of the detrimental effects of mechanical stresses and strains, some defects worsen as temperatures are lowered [1] and partially offset the predicted improvements. Second, refrigeration permits chips to retain functions that might otherwise become degraded when chip temperatures become excessive as chip heat fluxes extend beyond the limits of air-cooling capabilities. The advantages and disadvantages of using refrigeration to cool computers is reviewed further in a paper by Schmidt et al. [2].

 $^{^{2}}$ This estimate, which is based on limited data, assumes a uniform improvement in performance as the chip operating temperature is decreased.

[©]Copyright 2002 by International Business Machines Corporation. Copying in printed form for private use is permitted without payment of royalty provided that (1) each reproduction is done without alteration and (2) the Journal reference and IBM copyright notice are included on the first page. The title and abstract, but no other portions, of this paper may be copied or distributed royalty free without further permission by computer-based and other information-service systems. Permission to republish any other portion of this paper must be obtained from the Editor.

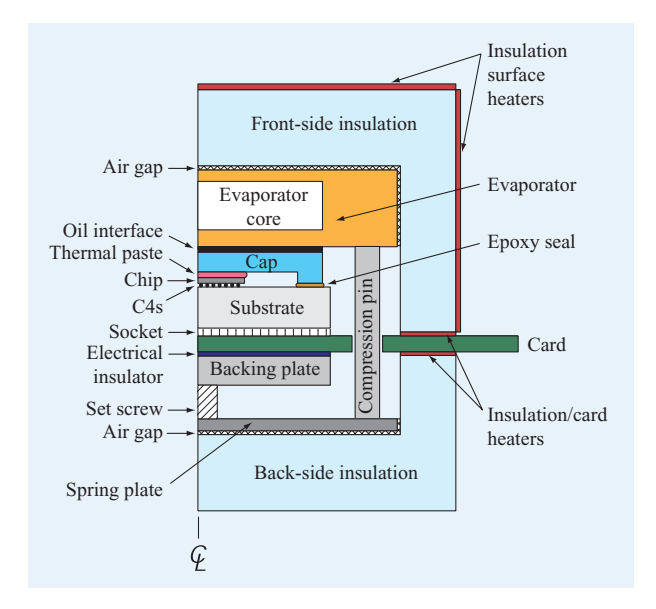


Figure '

Cross section (half-symmetry) of the low-temperature module/card assembly (not to scale).

years [3–7]. In September 1997, IBM began shipping its largest S/390* servers with refrigeration [8, 9]. This paper is an investigation of some of the key parameters that affect the thermal packaging design of a low-temperature-cooled single-chip module mounted on a printed circuit card. The effect of insulation properties and the environment surrounding such a module is explored using finite element modeling.

Description of physical model

The package that is modeled is a processor module card similar to the card currently shipped in IBM RS/6000* workstations. To minimize changes in mounting hardware or cards, the module card attachment scheme used in the current (air-cooled) product is used for this analysis of the refrigeration-cooled module. The processor is packaged in a 42.5-mm by 42.5-mm single-chip module (SCM) that dissipates 40 W during operation (see Figure 1). The chip is joined to an alumina substrate by an array of solder balls, called controlled collapse chip connections (C4s). The top surface of the module is encapsulated with an aluminum cap that is joined with an epoxy adhesive to the substrate. The heat removal is primarily from the back side of the chip to the cap through a thin layer of compliant thermal paste, then through a thin oil interface, and finally into the evaporator (a heat sink). The module is electrically connected to the card via a Thomas and Betts pressure-contact socket, with an array of conducting elastomeric contacts. The socket requires a compressive

force to function properly. A threaded set screw makes contact with the backing plate through the center of the spring plate. As the set screw is torqued to specification, the backing plate is pushed toward the card and the spring plate is pushed away from the card. Four stainless steel pins, located at the corners of the evaporator, protrude downward through the card and interlock with the spring plate. The evaporator is therefore pulled toward the front side of the card as the spring plate is pushed away from the back side of the card; the result is a socket squeezed between the module and the card.

Insulation surrounds the assembly on both the front and back of the card. An air gap of 0.5 mm is maintained between the evaporator spring plate and the insulation. In this model, heaters are selectively located to maintain surface temperatures above the dew point to prevent condensation (Figure 1). To raise the card surface temperature, heaters are placed under the perimeter of the insulation on the assembly. As shown below, additional heaters are required on the outer surfaces of the front-side insulation. Geometric and thermal properties for the different elements of the assembly are listed in **Table 1**.

As noted in Table 1, the roles of the insulation thickness and insulation conductivity in thermally isolating the assembly are investigated. For this low-temperature application, only those variables were evaluated which were of most interest and could be most easily applied. As previously stated, the objective of the design is to maintain all external surface temperatures above the dew point in order to prevent condensation. In addition to the insulation, combinations of boundary conditions in three other areas were examined:

- Heaters: adjacent to card top and bottom, and adjacent to the insulation top and sides.
- Ambient air temperatures: 25°C and 40°C.
- Convective boundary condition: 10, 20, and 50 W/m²K.

Model formulation and analysis

The ANSYS** Version 5.4 program was used to analyze a three-dimensional finite element model comprising thermal solid eight-node brick elements (SOLID70) (Figure 2). Steady-state thermal conduction was assumed in the module card assembly. As shown in Figure 2, quarter-symmetry of the assembly was utilized.

Many of the thermal conductivities listed in Table 2 (shown later) were obtained from available literature [10, 11]. The thermal conductivity of the glass-epoxy electrical insulator (Figure 1) was obtained from FR4 measurements made by Graebner and Azar [12]. The orthogonal thermal conductivities for the card, obtained from measurements made by Graebner and Azar, are defined by Equations (1) and (2):

$$K_x = K_y = 385 \left(\frac{z_{\text{Cu}}}{z}\right) + 0.87,$$
 (1)

$$K_z = \left[3.23 \left(1 - \frac{z_{\text{Cu}}}{z} \right) + 0.0026 \left(\frac{z_{\text{Cu}}}{z} \right) \right]^{-1},$$
 (2)

where K_x and K_y are the thermal conductivities (W/mK) parallel to the plane of the card (x and y directions), and K_z is the thermal conductivity (W/mK) perpendicular to the plane of the card (z direction), $z_{\rm Cu}$ is the total thickness of all continuous layers of copper (i.e., power planes), and z is the overall card thickness. The card contains eight signal planes and eight power planes, with a $z_{\rm Cu}$ of 0.244 mm (9.6 mils) and a z of 2.24 mm (88.3 mils).

There are three interface regions: 1) the poly-a-olefin (PAO) oil (a synthetic oil) interface between the evaporator and module cap; 2) the first-level solder ball array that joins the chip to the substrate (C4); and 3) the second-level connector array that attaches the module to the card (socket). Each interface is approximated by a one-dimensional thermal resistance. Since the heat flow through these interfaces is in the z direction, K_z is the effective thermal conductivity corresponding to the thermal resistance of the interface, and K_x and K_y are nullified. Defining the PAO oil interface is the most

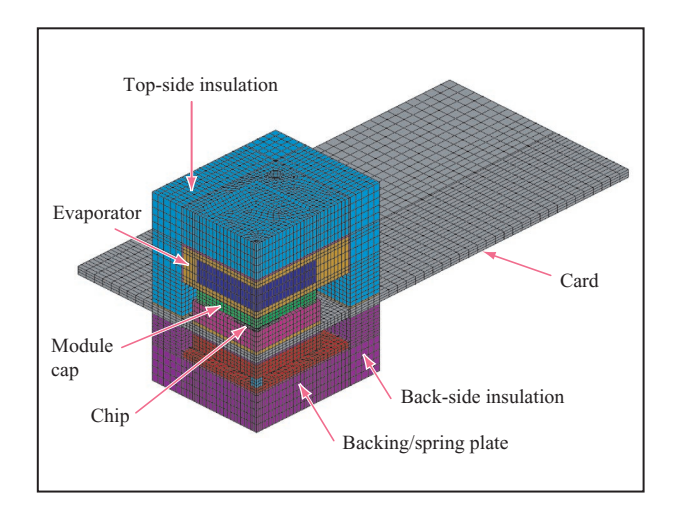


Figure 2

Three-dimensional finite element model (FEM) of module/card assembly (quarter symmetry).

straightforward. The oil, with a thermal conductivity of 0.18 W/mK, fills the microgaps formed when two surfaces are in contact with one another. The thickness of these microgaps corresponds to the roughness of the contacting

 Table 1
 Low-temperature module/card material characteristics.

Item	Material	Characteristic xy	Characteristic	Orthogonal thermal conductivity (W/mK)			
		dimensions (mm)	z/thickness (mm)	K_{x}	$K_{_{y}}$	K_z	
Spring plate	Low-carbon steel	61.8 × 49.1	1.6	46.7	46.7	46.7	
Backing plate	Low-carbon steel	42.5×42.5	3.8	46.7	46.7	46.7	
Compression pin (diameter)	Stainless steel	1.4	16.56	17	17	17	
Insulator	Glass epoxy	42.5×42.5	0.56	0.87	0.87	0.31	
Card	FR4/Cu	250×120	2.1	42.73	42.73	0.3473	
Socket	_	42.5×42.5	_	10^{-6}	10^{-6}	0.7162	
Substrate	Alumina (Al ₂ O ₃)	42.5×42.5	5.4	25	25	25	
Chip	Silicon	15.0×15.0	0.75	129	129	129	
Chip interconnect (C4)	95/5 PbSn solder	_	_	10^{-6}	10^{-6}	5.51	
Thermal paste	ATC 3.8	15×15	0.15	3.42	3.42	3.42	
Module cap	Aluminum 6061	40×40	2.6 above chip	180	180	180	
Oil interface	PAO oil	40×40	0.001	10^{-6}	10^{-6}	18	
Evaporator	OFCU	61.8×49.1	10.0	390	390	390	
Insulation	Polyurethane foam	_	10, 20	0.05, 0.1	0.05, 0.1	0.05, 0.1	
Heaters	Kovar	_	0.5	0.2	0.2	0.2	
Air gap	Air	_	0.5	0.024	0.024	0.024	
Cap epoxy	Loctite	_	0.1	0.7	0.7	0.7	

Table 2 Results for analyses involving only front-side insulation (no back-side insulation).

Case	Description	Convective boundary condition*	Insulation thickness (mm)	Insulation thermal conductivity (W/mK)	Minimum component temperature (°C)			Total refrigeration
					Exposed card surface	Front-side insulation (top center)	Backing plate	heat load (W)
1	Baseline	10/25	10	0.05	-9.0	4.8	-10.6	54.9
2	Higher convective boundary condition	50/25	10	0.05	5.1	18.0	6.4	59.6
3	Thicker insulation	10/25	20	0.05	-9.9	-4.8	-10.3	53.1
4	Higher convective boundary condition + thicker insulation	20/25	20	0.05	-16.8	13	-2.5	56.1
5	Heater between front-side insulation and card (30 W)	10/25	10	0.05	17.1	4.8	11.6	70.1
6	Heater between front-side insulation and card (20 W) + heater between card and backing plate (10 W)	10/25	10	0.05	25.0	4.8	28.0	69.0
7	Heater between front-side insulation and card (15 W) + heater between card and backing plate (7.5 W) + heaters on front-side insulation outer surface (4 W)	10/25	10	0.05	16.9	27.8	18.5	65.9

^{*}Heat transfer coefficient (W/m2K)/ambient temperature (°C).

surfaces and translates to an effective gap of 1 $\mu m.$ Nevertheless, since the elements in the model are contained in a 0.1-mm-thick region, providing an equivalent thermal resistance (i.e., the change in temperature per unit of heat flow) requires the thermal conductivity of the oil in the model to be 18 W/mK.

Computing the effective thermal conductivities for the solder and connector arrays was a little more complex. In both cases the thermal resistance of a single I/O connection was estimated and then scaled to the total interconnect area. The thermal resistance for the first-level solder array (approximately 3600 solder balls) was calculated to be 0.0807°C/W. The effective thermal conductivity for use in the model is therefore 5.508 W/mK, given an interfacial region in the model that is 0.1 mm thick. Finally, the thermal resistance of the socket is 0.773°C/W per contact. For 1077 contacts and a 1-mm-thick interfacial region in the model, the effective thermal conductivity of the socket used in the model is 0.7162 W/mK.

Model validation

Since experimental thermal data for this system was not available, the model was validated by comparison with a different thermal analysis program. The purpose of the validation was to ensure that the conduction model (with its complex material and geometrical entities) was accurate. It is not a validation of the assumptions that were used to arrive at the numerical model.

A three-dimensional finite element model using I-DEAS-ESC** Version 6a was developed. In this model, all interfacial resistances were handled by means of thermocoupling, a powerful method for generating paths for heat to flow between elements which do not share common nodes. The couplings are established on the basis of proximity, and can be distributed to account for overlap. In this technique, the magnitude of the couplings can be a fixed value or proportional to element surface area. A large number of heat-transfer processes can be accurately and efficiently modeled, including conduction, radiation, convection, and interface conductance. This feature can be used to conveniently and accurately create a thermal assembly of independently meshed model segments. To create the thermal coupling, ESC subdivides each primary element and establishes a conductance between each of these subelements and the geometrically nearest element in the secondary group. The magnitude of the conductances is based on the surface area of the primary sub-elements. ESC then merges the sub-elements back into the primary element and combines all parallel conductances, resulting in areaproportional thermal couplings that are correctly distributed among the nearest secondary elements, accounting for overlap. The heat transfer at the interface can be characterized by an effective heat-transfer coefficient value, h (W/m 2 K), and area-proportional conductances can thus be generated to join the two objects.

Using thermocoupling, this model obtains the thermal resistance due to the following resistances:

- Backing plate to card (glass epoxy).
- Card to substrate (socket).
- Substrate to chip (solder array or C4s).
- Substrate to cap (epoxy).
- Cap to evaporator (oil).
- Card to pin (air).

The ANSYS and I-DEAS analysis methods were compared for the case without insulation on the back side of the card. Since temperatures predicted by the two analyses differed by less than 2%, all subsequent runs used only ANSYS.

Results and discussion

Fifteen case runs were considered in the evaluation of the various design options available to maintain all exposed surfaces above the dew point. Also, it was desirable to minimize the total system power and total heat load on the refrigeration system, including heat loads which may be required by heaters in maintaining the temperatures of all external surfaces above the dew point. (For this study, 18°C was selected as the minimum dew point to simulate normal room environmental conditions.) These studies were not meant to be all-inclusive, but rather to provide an outline of the areas to consider in order to prevent condensation on exposed surfaces.

Five design options were investigated: insulation thickness, insulation thermal conductivity, room temperature, the external surface-convective heat-transfer coefficient, and the addition of heaters on external surfaces. To aid in the description of the results, temperatures were calculated and reported at four key locations, as shown in Figure 1; these are the card area outside the insulation, the center of the insulated box surrounding the module, the center of the insulated box surrounding the backing plate, and the backing plate. The lowest temperature for these locations is used when describing and contrasting the case studies.

Two design families were analyzed. The first had no insulation surrounding the backing plate on the back side of the card, since space constraints in some crowded systems will not permit it. The second design family used insulation surrounding the backing plate. The following sections consider the two design families, using the four calculated temperatures as guidance to the goodness of the results.

No insulation on back side of card

Baseline case

At the front of the card, 10-mm-thick insulation (such as polyurethane foam) with a thermal conductivity of 0.05 W/mK surrounded the module. An external convective boundary condition of 10 W/m²K with an

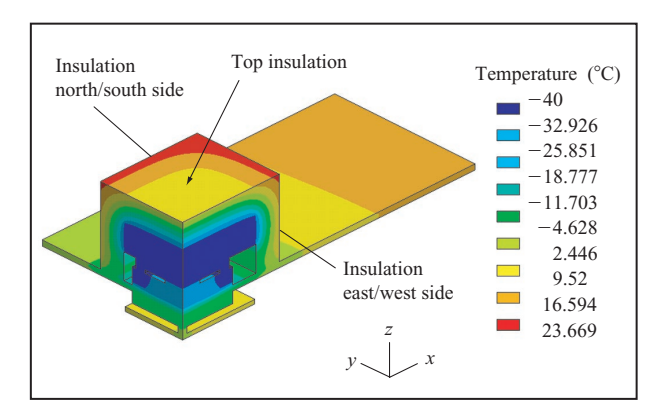


Figure 3

Finite element analysis showing three-dimensional contour mapping of temperatures on surfaces of module/card assembly (quarter symmetry) with front-side insulation. Baseline case (case 1).

ambient temperature of 25°C was used in the analysis. These parameters are typical for an air-cooled workstation environment.

The results for all of the cases involving only front-side insulation are reported in **Table 2**. The baseline case (case 1) showed that all four key locations would have temperatures well below the 18°C dew point criterion, so condensation would occur. A surface temperature contour map for the entire module card is shown in **Figure 3**. Contour maps are also shown for the front and back exposed areas of the card and for the front-side insulation in **Figures 4(a)**, **4(b)**, and **4(c)**, respectively.

Also note that the total refrigeration heat load of 54.9 W was 14.9 W (37.3%) greater than the active (module) heat load of 40 W. This additional heat load, typically referred to as a parasitic heat load, is due to heat that is transferred by virtue of the difference in temperature between the ambient air and the evaporator. This heat load must be accounted for when sizing the refrigeration system, and it should be kept to a minimum.

Effect of ambient boundary conditions

A convective boundary condition of 10 W/m²K would be reasonable for most workstation environments. One way to potentially increase surface temperatures above the dew point is to force ambient air over the module card. To simulate this behavior in the model, we increased the convective boundary condition to 50 W/m²K and kept the ambient temperature at 25°C. This increase in the ambient convective boundary condition yields the results tabulated in Table 2, case 2. These values show significant improvement in temperature compared to the baseline case, but the card and backing plate were still well below

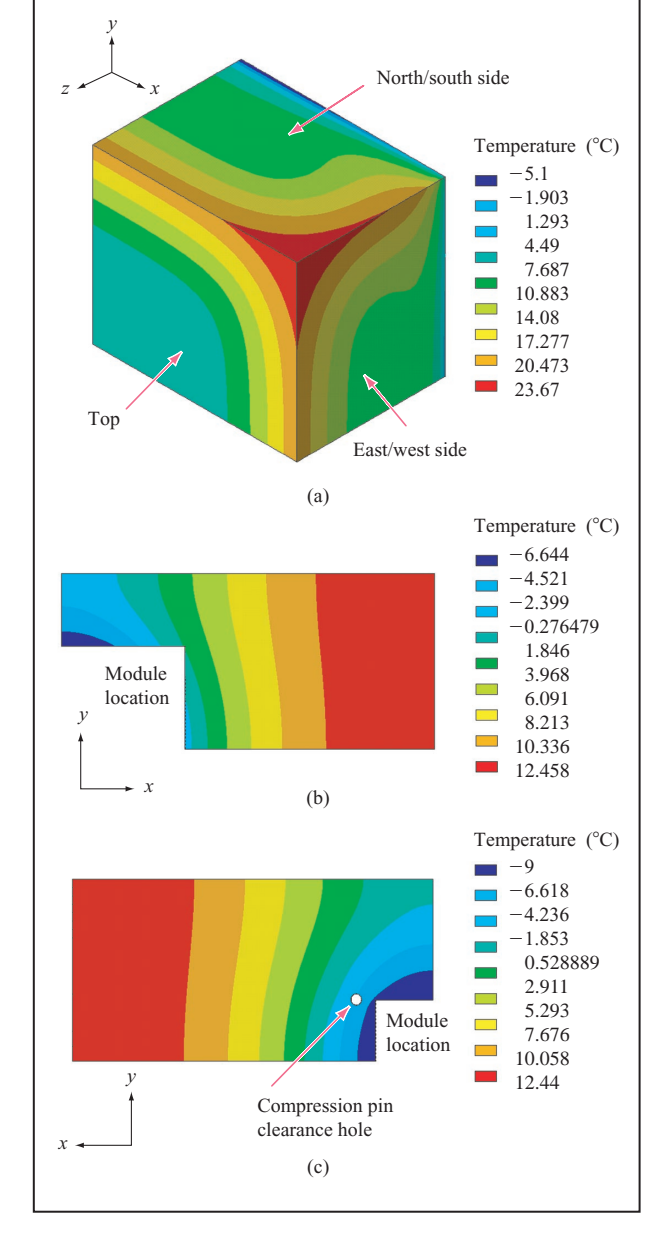


Figure 4

Contour maps derived from finite element analyses of particular areas of the module/card assembly shown in Figure 3. Temperatures at (a) front side of the exposed card surface; (b) back side of the exposed card surface; (c) surface of front-side insulation.

the dew point, and condensation would occur. The thermal path from the cold evaporator to the external ambient sink was greatly altered in this study compared to the baseline case. The temperature difference from source to sink was 65°C (25°C to -40°C) and with a larger convective heat-transfer condition and a resulting lower thermal resistance path compared to the baseline case, the

surface temperatures tended to approach the ambient temperatures more closely.

Effect of insulation thickness

Thicker insulation may be a viable option if space permits. The thickness of the insulation was increased from 10 mm to 20 mm with a convective boundary condition of 10 W/m²K and an ambient temperature of 25°C. The results are tabulated in Table 2, case 3. Surprisingly, this produced no appreciable change compared to the baseline case. As another option, the convective boundary condition was increased from 10 to 20 W/m²K in addition to the thicker insulation (20 mm). As shown by the results tabulated in Table 2, case 4, some temperatures increased while others decreased.

Effect of heaters adjacent to board

Since neither thicker insulation nor improved convective boundary conditions increased the temperature of exposed surfaces above the dew point, heaters were added. In this first case, a heater (30 W) was added to the front side of the card at the interface between the card and the base of the insulation. All other conditions were the same as the baseline case. The key results are tabulated in Table 2, case 5. Although these temperatures were much higher than for any case discussed so far, temperatures remained below the dew point and were considerably below at the center of the insulation. Note that the additional heat input (30 W) was transferred to the refrigeration system.

The heat input at the interface of the top insulated box and the card was not adequate to raise all key temperatures above the dew point. Therefore, in the next case a back-side heater was added between the card and backing plate (in place of the electric insulator) in addition to the front-side heater. The results obtained when 20 W was applied to the front heater and 10 W to the back heater are tabulated in Table 2, case 6. The results were promising in that the temperatures of all exposed surfaces of the card and the backing plate rose above the dew point. However, the top of the insulated box was still below the dew point.

As a final step, heat was added to the surfaces of the insulated box. A total of 4 W was applied, 2 W on the top and 2 W on the sides of the box. Almost all conditions were the same as in the prior case, except that the heat input at the interface of the backing plate with the card was reduced from 10 W to 7.5 W, and the heat input at the interface of the insulation with the card was reduced from 20 W to 15 W.

The results (Table 2, case 7) show that the temperature of the insulation box had risen above the dew point, and that the card and backing plate were near, though still somewhat below, the dew point. Since the previous case had shown that 20 W and 10 W on the heaters adjacent to

Table 3 Results for analyses involving both front-side and back-side insulation.

Case	Description	Convective boundary condition*	Insulation thickness (mm)	Insulation thermal conductivity (W/mK)	Minimum component temperature (°C)			Total refrigeration
					Exposed card surface	Front-side insulation (top center)	Backing plate	heat load (W)
8	Baseline	10/25	10	0.05	-9.1	4.8	13.4	52.4
9	Heater between front-side insulation and card (15 W) + heater between back-side insulation and card (10 W)	10/25	10	0.05	25.0	4.8	18.7	65.0
10	Heater between front-side insulation and card (15 W) + heater between back-side insulation and card (10 W) + heaters on front-side insulation outer surfaces (4 W)	10/25	10	0.05	25.5	27.9	18.7	65.8
11	Case 10 with higher insulation thermal conductivity	20/25	20	0.10	25.0	14.7	17.1	67.1

^{*}Heat-transfer coefficient (W/m2K)/ambient temperature (°C).

the card resolved the card and backing plate temperatures, a slight increase in these heat inputs would resolve this case. The total heat input for this case was 26.5 W with a refrigeration load of 65.9 W. It is expected that a total heat input of approximately 30 W would resolve the low temperatures on the card and backing plate. This is a solution to the problem for the case in which insulation is not allowed on the back side of the card.

The following sections discuss the second design option, in which insulation is added to the back side of the card when space in the workstation permits it.

Insulation on back side of card

Baseline case

All physical and boundary conditions for this case were the same as for the baseline case with insulation only around the module, except that insulation was added to the back side of the card. The insulation surrounding both the module and backing plate was 10 mm thick, with a thermal conductivity of 0.05 W/mK. An external convective boundary condition of 10 W/m²K with an ambient temperature of 25°C was used in the analysis. This baseline case (**Table 3**, case 8) does not differ appreciably from the baseline case without back-side insulation (Table 2, case 1).

Now, when considering back-side surface temperatures, the backing plate is no longer an exposed surface. The back-side insulation (bottom center thermocouple) temperature is therefore the key temperature measurement for condensation.

Effect of heaters

Since insulation by itself on the back side of the card did not eliminate the dew point problem, heaters were considered. A back-side card heater was placed between the card and the back-side insulation instead of between the card and backing plate. The first case examined was with the front-side card heater at 15 W and the back-side card heater at 10 W. All other conditions were kept the same as the baseline case. The results (Table 3, case 9) show that the card and bottom insulation temperatures were above the dew point; only the top insulation surrounding the module remained below the dew point.

In case 10, heat was added to the surfaces of the top insulated box. As in case 7, these heaters added 2 W on the top and 2 W on the sides of the box. The results (Table 3, case 10) show that all key temperature monitoring points met the condensation criterion that all surfaces be above 18°C.

Effect of insulation thermal conductivity

The effect of higher insulation conductivity on temperature was evaluated and is shown in Table 3, case 11. This is similar to case 10, except that the thermal conductivity of the insulation was increased by a factor of 2 (from 0.05 W/mK to 0.10 W/mK). Several comments can be made about the effect of the thermal conductivity properties of the insulation. The first is that the card surface temperature changed very little and was still above the dew point temperature limit. Second, the top-side insulation fell below the dew point temperature, but could easily be corrected with the addition of a slight amount of heat (estimated at about 5 W) to the insulation surfaces.

Finally, the heat load on the refrigeration system increased to some extent. These results are important in that it appears that if the insulation thermal conductivity falls within a reasonable range, the results are not significantly affected.

Summary and conclusions

A finite element analysis of control of a cooled singlechip electronic module to minimize local condensation at temperatures below the dew point was investigated. Five parameters were examined to determine their effect on eliminating condensation on any exposed surfaces. Two design options consistent with the spatial constraints of most workstations were considered. One option considered only the insulation on an assembly that surrounds the module, with heaters added as required to maintain temperatures above the dew point; the second option introduced insulation onto the back side of the card in addition to the heaters. Both designs were shown to be viable, with the same number of heated surfaces required, and the additional refrigeration heat load was almost identical for the two options. The design option without additional insulation on the back side of the card would therefore be best, since it decreases the number of parts required.

Finally, the change in the insulation surface temperature effected by modifying either the convective or conduction thermal resistance path from the cold evaporator to the ambient temperature sink was studied. As expected, a decrease in insulation thermal conductivity and/or an increase in convective heat transfer increases the surface temperatures.

- *Trademark or registered trademark of International Business Machines Corporation.
- **Trademark or registered trademark of ANSYS, Inc. or Structural Dynamics Research Corporation.

References

- 1. W. Needham, C. Prunty, and E. H. Yeoh, "High Volume Microprocessor Test Escapes, an Analysis of Defects Our Tests Are Missing," *Proceedings of the IEEE International Test Conference*, 1998, pp. 25–34.
- R. R. Schmidt, M. J. Ellsworth, Jr., R. C. Chu, and D. Agonafer, "Refrigeration Cooled Computers: Application and Review," *Proceedings of the International Mechanical Engineering Congress and Exposition 2000*, Orlando, FL, November 5–10, 2000, pp. 277–283.
- KryoTech and Digital Release 767 MHz Workstation, news release presented at the National Association of Broadcasters (NAB) Conference, Las Vegas, April 6, 1998.
- 4. S. Brody, "Cold Computing Has Arrived," Supercond. & Cryoelectron. 11, No. 2, 29-33 (1998); see http://www.superconductorweek.com/scce/backissues.htm.
- 5. Proceedings of the 35th Design Automation Conference (DAC), San Francisco, June 15–19, 1998.
- M. F. W. Brown, G. M. Chrysler, J. G. Maveety, and E. A. Sanchez, "Thermal Management for Electronics Cooling Using a Miniature Compressor," presented at

- M-CAIC III—Military and Commercial Applications for Low-Cost Cryocoolers, San Diego, October 25–26, 2001.
- R. Schmidt, "Low Temperature Electronic Cooling," *Electron. Cooling* 6, No. 3, 18–24 (September 2000).
- 8. IBM G4 announcement letter 197-127, June 9, 1997; see http://www2.ibmlink.ibm.com.cgi-bin/master?xh = cM*OKpqdq9m\$u42USenGnN9332&request = announcements&parms=H%5f197%2d127&xhi=usa%2emain&xfr=N.
- 9. P. J. Singh, W. D. Becker, V. Cozzolino, M. J. Ellsworth, Jr., R. R. Schmidt, and E. J. Seminaro, "System Packaging of a CMOS Mainframe," *Adv. Microelectron.* **25**, No. 7, 14–19 (1998).
- R. R. Tummala and E. J. Rymaszewski, Eds., Microelectronics Packaging Handbook, Van Nostrand Reinhold, New York, 1989, p. 173.
- 11. F. P. Incopera and D. P. DeWitt, *Fundamentals of Heat and Mass Transfer*, Third Edition, John Wiley and Sons, Inc., New York, 1990, pp. A3–A6.
- J. E. Graebner and K. Azar, "Thermal Conductivity Measurements in Printed Wiring Boards," J. Heat Transfer 119, No. 3, 401-405 (August 1997).

Received June 17, 2001; accepted for publication May 22, 2002

Michael J. Ellsworth, Jr. IBM Server Group, 2455 South Road, Poughkeepsie, New York 12601 (mje@us.ibm.com). Mr. Ellsworth is a Senior Technical Staff Member working in the IBM Advanced Thermal Laboratory in Poughkeepsie, New York. He received his B.E.M.E. degree (1984) and his M.E.M.E. degree (1988) from Manhattan College, Riverdale, New York, joining IBM in 1988. While at IBM he has explored improved cooling for applications ranging from laptops to high-end servers and has investigated cooling technologies encompassing air, water, and refrigeration. From 1992 to 1996 he was a ceramic/thin-film package applications engineer and technical program manager in the IBM Interconnect Products Group in East Fishkill, New York. Mr. Ellsworth is a member of IEEE and of ASME, where he serves on the K16 Committee on Heat Transfer in Electronic Equipment. He has published 10 technical papers and holds 13 US patents. He is a registered Professional Engineer in the state of New York.

Roger R. Schmidt IBM Server Group, 2455 South Road, Poughkeepsie, New York 12601 (c28rrs@us.ibm.com). Dr. Schmidt is a Distinguished Engineer, a member of the IBM Academy of Technology, and an ASME Fellow. He received his B.S. degree in mechanical engineering from Bradley University and his M.S. and Ph.D. degrees in mechanical engineering from the University of Minnesota. Dr. Schmidt has more than 25 years' experience in engineering and engineering management in the thermal design of IBM largescale computers. He has led development teams in cooling mainframes, client/servers, parallel processors and test equipment utilizing such cooling mediums as air, water, and refrigerants. Dr. Schmidt has published more than 50 technical papers, and he holds 33 patents in the area of electronic cooling. He is a member of the ASME Heat Transfer Division and an active member of the ASME K-16 Electronic Cooling Committee, and is an Associate Editor of the Journal of Electronic Packaging. Over the past 15 years, Dr. Schmidt has taught many mechanical engineering courses for prospective Professional Engineers; he has given seminars on electronic cooling at several universities.

Dereje Agonafer Electronics, MEMS, and Telecommunications Systems Packaging Center, University of Texas, 500 West First Street, Arlington, Texas 76019 (agonafer@uta.edu). Dr. Agonafer is Professor and Director of the Electronics, MEMS, and Telecommunications Systems Packaging Center at the University of Texas at Arlington. He joined UTA after 15 years' experience in IBM, where he was the Center of Competence in the area of computer-aided thermal engineering. Research at the UTA EMTSP Center is multidisciplinary and includes such areas as electronic cooling, reliability, and electronic materials. Dr. Agonafer holds seven issued patents and has published extensively. He is Editor in Chief of the ASME Press Book Series in Electronic Packaging and Associate Technical Editor of the Journal of Electronic Packaging. Dr. Agonafer was chair of the ASME K-16 Electronic Cooling Committee (1997-2000) and ASME Electronics and Photonics Packaging Division Chair in 2000.